Journal of Membrane Science 590 (2019) 117295

Contents lists available at ScienceDirect

Journal of Membrane Science

journal homepage: www.elsevier.com/locate/memsci

Functional group configuration influences salt transport in desalination membrane materials

Hongxi Luo[1], Kevin Chang[1], Kevin Bahati, Geoffrey M. Geise[*]

Department of Chemical Engineering, University of Virginia, 102 Engineers' Way, P.O. Box 400741, Charlottesville, VA, 22904, USA

ARTICLE INFO

Keywords:
Dielectric
Permittivity
Water
Polymer
Permeability

ABSTRACT

Five methacrylate-based co-polymers, which have different ratios of 2-hydroxyethyl methacrylate (HEMA) and glycerol methacrylate (GMAOH) co-monomers, were prepared to investigate the influence of functional group configuration on salt transport properties. The HEMA and GMAOH co-monomers were selected because of the differences in position and number of hydroxyl groups in the two molecules. Co-polymer composition was varied systematically from a vicinal diol-rich (GMAOH-rich) configuration to a distributed hydroxyl group (HEMA-rich) configuration. To decouple the impact of functional group configuration and of changing water content on transport properties, all of the materials were prepared to have statistically equivalent water content. Salt sorption was lower and salt diffusion was slower in the HEMA-rich configuration compared to the GMAOH-rich configuration. Microwave dielectric relaxation spectroscopy revealed lower relative permittivity (i.e., dielectric constant) for the HEMA-rich co-polymers, which is consistent with suppressed salt sorption in those materials compared to the GMAOH-rich co-polymers. This observation was complemented by state of water analysis that suggested freezable (i.e., bulk-like) water content decreased as HEMA content increased. Both results suggest that stronger interactions between water molecules and the polymer are favored when hydrophilic functional groups are distributed more evenly throughout the material. These results suggest that functional group position in hydrated polymers influences salt transport properties, and engineering polymers that have a distributed functional group configuration may suppress salt transport properties, which could result in favorable materials for desalination membranes.

1. Introduction

Desalination is one strategy to improve access to clean water and address global water shortage [1–7]. Membrane-based desalination techniques, such as reverse osmosis, are widely used due to high energy efficiency and low cost compared to thermal desalination technologies [4,5,8–10]. The effectiveness of desalination membranes is intimately coupled to the water and salt transport properties of the polymer used to prepare the membrane, and materials that afford high water/salt selectivity, whether by enhancing water transport or by suppressing salt transport, are desirable for desalination applications [11,12].

Polyamide-based reverse osmosis membranes, with high water permeance and low salt passage, are the current state-of-the-art for membrane-based desalination [1,2,5,7]. Polyamides, however, are susceptible to oxidative degradation via chlorine-based chemicals used to disinfect water and to limit biofouling, so advanced chlorine-tolerant, or chemically stable, desalination membranes are needed [13–16]. Several candidate materials have been considered [4,5,16–18], but a combination of excellent chlorine tolerance and favorable water/salt selectivity properties remains elusive [11,12,19]. Engineering the next generation of desalination membranes with desirable combinations of transport properties, chemical and mechanical stability, and surface properties requires knowledge of how specific chemical functional groups influence material properties.

One approach to designing effective desalination membranes is to engineer polymers that suppress salt permeability. So long as water transport properties are not simultaneously suppressed to the same or greater extent, this approach would increase salt rejection [4,19,20]. The solution-diffusion model (for non-porous polymers such as those often used in desalination membranes) suggests that salt permeability can be suppressed by reducing salt partitioning (i.e., sorption) into the membrane and/or salt diffusion through the membrane as salt permeability is the product of salt sorption and diffusion [21,22].

In relatively simple uncharged hydrated polymers, salt sorption

[*] Corresponding author.
E-mail address: geise@virginia.edu (G.M. Geise).
[1] Authors contributed equally to this work.

https://doi.org/10.1016/j.memsci.2019.117295
Received 1 February 2019; Received in revised form 18 July 2019; Accepted 21 July 2019
Available online 22 July 2019
0376-7388/

properties are linked to the relative permittivity (or dielectric constant) of the material [19,23–25], and polymer chemistry can be used to engineer relative permittivity to influence the thermodynamics of salt sorption [23]. Additionally, preparing membranes (with low water content – similar to desalination membranes) with rigid polymer backbones and/or bulky side groups can result in favorable water/salt transport selectivity [26–28]. These findings inform opportunities to engineer polymers to achieve the necessary combination of properties to purify water effectively.

One challenge in many fundamental studies of membrane transport properties is that modification of the polymer often changes the hydrophilicity of the material [4–6,29]. In other words, a change in water content often accompanies systematic variations in polymer chemistry. Water content can have a profound impact on the water and salt transport properties of polymers [4,19,30–32], and it can be difficult to decouple the influences of changing water content and polymer chemistry on transport properties. Doing so, however, is critical to understanding how molecular engineering can be used to design advanced membrane materials.

Here we prepared five methacrylate-based co-polymers that have statistically equivalent water content but different ratios of two co-monomers that have different numbers of hydroxyl groups: 2-hydroxyethyl methacrylate (HEMA) and glycerol methacrylate (GMAOH). Selecting these co-monomers enabled a systematic variation of the position and number density of hydroxyl groups in the co-polymers without changing the water content of the material. The chemical composition of the co-polymer was systematically varied from a vicinal diol-rich configuration (GMAOH-rich co-polymer) to a HEMA-rich material with single hydroxyl groups on the side chains. Shifting the co-polymer composition from a GMAOH-rich configuration to a HEMA-rich configuration suppressed both salt sorption and salt diffusion properties, and these results were supported by dielectric permittivity property measurements and state of water analysis. The results suggest, without complication from changing water content, that a more distributed hydrophilic functional group configuration may suppress salt transport to a greater extent than a more vicinal functional group-rich configuration within the co-polymer. As such, this study provides information about how specific chemical functional groups influence salt transport properties in a unique manner that is decoupled from polymer water content.

2. Experimental methods

2.1. Materials

Co-polymers (Fig. 1) were prepared by photo-initiated cross-linking of 2-hydroxyethyl methacrylate (HEMA, 99%, Sigma-Aldrich, St. Louis, MO), glycidyl methacrylate (GMA, 97%, Sigma-Aldrich, St, Louis, MO), and glycerol methacrylate (GMAOH, synthesized as reported by Tan et al. [33]). The cross-linker was poly(ethylene glycol) dimethacrylate (PEGDMA, average Mn = 550 g/mol, Sigma-Aldrich, St. Louis, MO). The cross-linker content (10% of the total mass of the co-monomers) was chosen to mitigate two competing objectives: minimizing the cross-linker content to study the influence of co-monomer functionality on transport properties while incorporating enough cross-linker to yield mechanically robust materials. The initiator was 1-hydroxycyclohexyl phenyl ketone (HCPK, 99%, Sigma-Aldrich, St. Louis, MO), and the amount of initiator used was 1% of the total co-monomer mass [26,27].

In a typical preparation of the 15:55:30 HEMA:GMA:GMAOH material, 0.15 g of HEMA, 0.55 g of GMA, 0.3 g of GMAOH, 0.1 g of PEGDMA, and 10 mg of HCPK were mixed, via magnetic stirring, in a 20 mL glass vial. The mixture was stirred at room temperature for 30 min and then was degassed for 10 min in an ultrasonic bath (VWR, 97043). The result of this process was a homogeneous and bubble-free pre-polymerization solution.

This solution subsequently was deposited slowly onto a clean glass

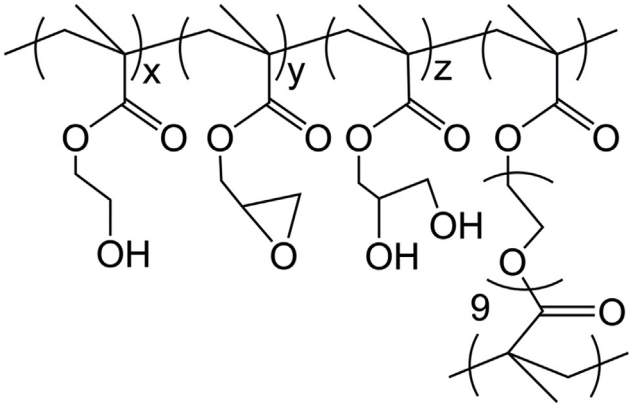

Fig. 1. Chemical structure of the cross-linked HEMA:GMA:GMAOH co-polymer. The co-polymers were prepared from pre-polymerization solutions that contained a x:y:z, by mass, ratio of HEMA:GMA:GMAOH co-monomers (such that x + y + z = 100). The cross-linker was added such that the mass of cross-linker was 10% of the total mass of the co-monomers.

plate. Two 100 μm thick metal spacers were placed on either side of the solution, and a quartz plate was placed on top of the spacers to create a uniformly thick film of the pre-polymerization solution. This assembly was placed on a leveled platform in a UV-crosslinking chamber (Spectroline, Select™ Series). The pre-polymerization solution was irradiated with 120 μJ/cm^2 312 nm light for 5 min, which was sufficiently long to form mechanically robust membranes, to obtain a colorless and transparent membrane film.

The transparent nature of the films was an indicator that the materials are relatively homogeneous. Glass transition temperatures can also provide additional information about the morphology of these dense thick films [34]. Homogeneous co-polymers, i.e., materials where the co-monomers are well-mixed at the molecular level, are expected to exhibit a single glass transition temperature [26,34]. Unfortunately, the glass transition temperatures of all of the HEMA:GMA:GMAOH co-polymers appear to be obscured by vaporization of some of the water initially sorbed by the co-polymer. The Fox equation [35,36], which can be used to calculate a first approximation estimate of the co-polymer glass transition temperature based on homopolymer glass transition temperatures and co-polymer composition, provides evidence for this situation. Furthermore, the Fox equation has been used to calculate values in good agreement with experimentally measured glass transition temperatures for HEMA-containing materials [27]. The Fox equation estimated hydrated co-polymer glass transition temperatures increased in the order of 108 °C, 113 °C, 116 °C, 121 °C, and 126 °C as the HEMA composition of the pre-polymerization solution increased from 0 to 60% (by mass). Importantly, we did not observe glass transition temperatures at the temperatures where a glass transition would be expected if the co-monomers were prepared as homopolymers, and this result further suggests that the co-polymers were relatively homogeneous. As such, the transparent nature of the films and the glass transition temperature data/analysis suggest that the co-polymers considered here are relatively homogeneous.

Following the cross-linking process, the membrane was removed carefully from the surface and immersed in de-ionized (DI) water (18.2 MΩ cm). Five materials, with different ratios of the co-monomers (Fig. 2), were prepared using this process. The mass composition of the pre-polymerization solution used to prepare the co-polymers was used to distinguish the materials, and Fourier-transform infrared (FT-IR) spectroscopy (see Supplementary Information and Fig. S1) suggests that the pre-polymerization solution composition is representative of the composition of these cross-linked networks. All materials were stored in DI water until use.

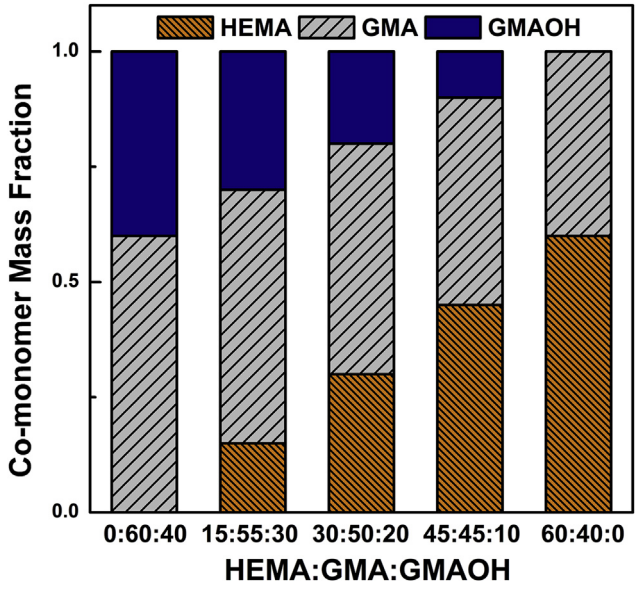

Fig. 2. The co-monomer content of the co-polymer was systematically varied (by adjusting the composition of the pre-polymerization solution used to prepare the co-polymers) to probe the influence of hydroxyl group configuration on the salt transport properties of the five HEMA:GMA:GMAOH materials considered. The nomenclature on the horizontal axis corresponds to the pre-polymerization solution mass composition.

2.2. Methods

2.2.1. Water uptake

After an initial equilibration period of at least 48 h, samples were removed from the DI water. Residual surface water was wiped from the film, and the wet sample mass, m_w, was measured immediately thereafter. Samples were subsequently dried under vacuum at 22 ± 1 °C (ambient temperature) for at least 48 h to remove sorbed water. After drying, samples were removed quickly from the oven, and the dry mass, m_d, of the sample was measured. Pure water uptake, w_u, was calculated as:

$$w_u = \frac{m_w - m_d}{m_d} \tag{1}$$

Dry polymer density, ρ_p, was measured immediately after the dry mass measurement using an Archimedes' principle method [26–28,37,38]. The dry polymer density, ρ_p, was calculated as:

$$\rho_p = \frac{m_{air}}{m_{air} - m_{aux}}(\rho_{aux} - \rho_{air}) + \rho_{air} \tag{2}$$

where m_{air} was the sample mass measured in air, m_{aux} was the sample mass measured in an auxiliary liquid, ρ_{aux} was the auxiliary liquid density, and ρ_{air} was the air density. Cyclohexane was chosen as the auxiliary liquid [26–28], and the cyclohexane density was evaluated at the measurement temperature [39,40]. The cyclohexane uptake by all of the materials considered was measured to be less than 2% (by mass) over a 12 h period of time, which is considerably longer than the approximately 30 s density measurement.

Assuming volume additivity between sorbed water and polymer [4,41], the volume fraction of water sorbed in the polymer, φ_w, was determined as [4]:

$$\varphi_w = \frac{w_u}{w_u + \frac{\rho_w}{\rho_p}} \tag{3}$$

where ρ_w was taken as the density of water (1.0 g/cm^3 [39]). The value of φ_w is effectively equivalent to the water sorption coefficient, K_w, which is defined as the ratio of the concentration of water in the polymer to that in the bulk external solution [4,5,21,22].

2.2.2. Salt sorption

The partitioning of salt from an external solution into the polymer was characterized using a desorption method [20]. First, samples were equilibrated with 0.5 mol/L sodium chloride (NaCl) solution for at least 3 days. This equilibration time was well in excess of the characteristic time for salt diffusion, which was conservatively estimated as film thickness squared divided by measured salt permeability [20,42], in these materials. After equilibration, samples were removed from the salt solution, the residual surface solution was wiped quickly using laboratory wipes, sample thickness was measured using digital calipers (Mitutoyo, Item # 293–344), sample diameter was measured, and the sample was placed in 20 mL of DI water to allow sorbed salt in the sample to desorb from the polymer. The salt sorption coefficient, K_s, which is defined as the ratio of the salt concentration in the polymer relative to the salt concentration of the external solution in equilibrium with the polymer [20], was calculated as:

$$K_s = \frac{C_s^m}{C_s^s} = \frac{C_d V_d}{C_s^s V_p} \tag{4}$$

where C_s^m is the salt concentration in the polymer, C_s^s is the salt concentration in the initial external solution (i.e., 0.5 mol/L NaCl), C_d is the final salt concentration in the desorption solution, V_d is the desorption solution volume, and V_p is the volume of the hydrated polymer sample, which was determined geometrically using the average thickness and diameter of the circular sample coupon.

2.2.3. Salt transport

Salt permeability was characterized using a custom-built diffusion cell apparatus consisting of two jacketed chambers (i.e., donor and receiver chambers) that were separated by the sample. Silicone rubber gaskets were used to tightly seal the sample into the cell (i.e., to prevent leaks from the donor and/or receiver chambers). The donor chamber was filled with 100 mL of 0.5 mol/L NaCl solution, and the receiver chamber was filled with 100 mL of DI water. These solutions were stirred at a rate of 360 rpm using overhead mechanical stirrers to keep the solutions well mixed and minimize boundary layer effects.

The conductivity of the receiver chamber solution was recorded as a function of time using a conductivity meter (Cond 7310, WTW), and the solution temperature was maintained at 25 °C by circulating water through the chamber jackets using a water circulator with a temperature controller [43]. Conductivity was subsequently converted to salt concentration via a calibration curve. Salt permeability, P_s, was modeled as one-dimensional transient Fickian diffusion and was determined via a linear regression of the time-dependent salt concentration data in the form [26,31,43]:

$$-\frac{VL}{2A}\ln\left(1 - 2\frac{C_R(t)}{C_D(0)}\right) = P_s t \tag{5}$$

where V is the volume of liquid (i.e., salt solution or DI water) in the donor and receiver chambers, A is the sample area available for transport, t is time, $C_R(t)$ is the salt concentration in receiver chamber at time t, and $C_D(0)$ is the initial salt concentration in donor chamber (at $t = 0$). The measured salt permeability and salt sorption coefficients were used to calculate the apparent salt diffusion coefficient, D_s, as [4,5,21,22]:

$$D_s = \frac{P_s}{K_s} \tag{6}$$

2.2.4. Microwave dielectric relaxation spectroscopy

Hydrated polymer dielectric permittivity properties were characterized as the frequency-dependent relative complex permittivity ε^*[44,45], using a Keysight N9928A vector network analyzer (VNA) [23]. S-parameters, related to the relative complex permittivity, were measured over a frequency range of 450 MHz to 20 GHz using the VNA

[23]. Analysis software interpreted the measured S-parameters as the relative complex permittivity properties of the samples [21,23,46]. The VNA calibration and S-parameter analysis were performed as described previously [23]. The real part of the relative complex permittivity was the relative permittivity, ε', (often referred to as the dielectric constant) of the sample, and the imaginary part of the relative complex permittivity was the dielectric loss, ε'', of the sample [44].

A 5 cm long and 3.5 mm diameter coaxial transmission line or waveguide (Maury Microwave, catalog number 8043S5) was used as the sample holder. Shielded coaxial cables (Keysight Technologies, catalog number N9910X0-708) were used to connect the VNA and the transmission line. Co-polymer samples were carefully cut, using a razor blade, into small rectangular-shaped strips that were approximately 0.5 cm wide, and these strips were carefully and tightly wrapped around the inner conductor of the transmission line until sufficient polymer was wrapped to fill the annular space of the transmission line with the absence of air gaps.

2.2.5. State of water analysis

Differential scanning calorimetry (DSC, TA Instruments Q1000) was used to characterize the state of water sorbed in the materials. First, DI water equilibrated samples were loaded in well-sealed hermetic aluminum pans, which prevented water loss during the experiment. The samples were quenched to −70 °C in the DSC instrument and then scanned once from −70 °C to 90 °C at a heating rate of 10 °C/min. The DSC sample chamber was continuously purged with dry nitrogen during the experiment [26,27,47].

The results were analyzed to quantify the relative amounts of freezable (i.e., bulk-like, or weakly bound water) and non-freezable water (i.e., strongly bound water) in the co-polymer [23,48–56]. Freezable, w_f, and non-freezable, w_{nf}, water content were calculated as:

$$w_f(\%) = \frac{m_f}{m_d} \times 100\% = \frac{\Delta H_{polymer}}{\Delta H^{\circ}_{m,H_2O}} \times (w_u + 100) \tag{7}$$

$$w_{nf}(\%) = W_c - W_f \tag{8}$$

where m_f was the freezable water mass in the co-polymer, $\Delta H_{polymer}$ was the enthalpy of melting in the co-polymer determined by integrating the water melting peak (at 0 °C) measured using DSC, and $\Delta H^{\circ}_{m,H_2O}$ was the enthalpy of melting for water (333.5 J/g) [56].

3. Results and discussion

3.1. Water uptake

The primary goal of this study was to determine the influence of hydroxyl group configuration on salt transport properties. To accomplish this goal, five HEMA:GMA:GMAOH materials were prepared with different ratios of HEMA and GMAOH (Fig. 2), which have different numbers of hydroxyl groups (Fig. 1). As polymer water content critically affects the salt transport properties of hydrated polymers [4,31], it was important to prepare the materials used in this study such that the water content of all of the materials was statistically equivalent. By doing so, transport property differences between the materials can be ascribed to changes in the functional group configuration of the polymer without needing to consider the effect of changing water content.

Over the range of co-monomer compositions considered, a series of materials were prepared such that the water uptake and water sorption coefficient properties were statistically indistinguishable (Table 1). As the HEMA content of the co-polymer increased (and the GMAOH content of the co-polymer decreased), the overall hydroxyl group content in the co-polymer decreased by approximately 8%. We also observed similar dry density values for all co-polymers (Table 1), suggesting that the changing of functional group orientation does not significantly affect chain packing in the materials. As the HEMA content of the co-polymer increases, the cross-link density likely decreases to a small extent (estimated to be approximately 7% using the molar composition of the polymer [57]) to offset the small decrease in hydroxyl group content and yield a series of materials that have statistically indistinguishable water content (Table 1). It is also possible, however, that differences in the intrinsic hydrophilicity of the HEMA and GMAOH co-monomers may contribute to this balance. The water uptake of HEMA is reported to be 0.60 g(water)/g(dry polymer), and GMAOH is reported to be water soluble [26,33]. Additionally, molar enthalpy of mixing data for mixtures of water and either ethanol [58] or 1,2-propanediol [59], which are representative of the HEMA and GMAOH side chains, respectively, suggest that mixing of water and 1,2-propanediol is more thermodynamically favored compared to the situation for water and ethanol. If ethanol and 1,2-propanediol are taken to be representative of the side chains of HEMA and GMAOH, respectively, these results suggest that mixing of water and GMAOH may be more thermodynamically favored compared to that of water and HEMA [57]. Both analyses suggest that the GMAOH side chain is more hydrophilic compared to the HEMA side chain. Subsequent transport property data will be discussed within the framework of the co-monomer composition and hydroxyl group content of the co-polymer.

3.2. Salt transport properties

As the HEMA content of the polymer increases and the GMAOH content of the polymer decreases, the configuration of hydroxyl groups on the polymer side chains shifts from a vicinal diol-rich material (when the GMAOH content is high compared to HEMA) to a material where most side chains contain a single hydroxyl group (when the HEMA content is high compared to GMAOH). Therefore, we were able to use the HEMA:GMA:GMAOH materials to study the influence of hydroxyl group distribution on salt transport properties without concern for changing water content (as the water content of the HEMA:GMA:GMAOH series of materials was equivalent, Table 1). Salt transport properties can be engineered by controlling the molecular distribution of hydroxyl groups within the polymer, and this observation may have implications for molecular design of desalination membrane materials.

The co-monomer content of the materials was varied by adjusting the mass composition of the co-monomers in the pre-polymerization solution used to prepare the co-polymers. While Fourier transform infrared (FT-IR) spectroscopy (see Supplementary Information) indicates that the co-polymer composition reflects the pre-polymerization solution composition, the similar chemistry and cross-linked network architecture of the co-polymers impedes quantitative measurement of the co-polymer composition. The hydroxyl group content, reported in Table 1, was calculated from the pre-polymerization solution composition under the assumption that the pre-polymerization solution composition translates directly into the co-polymer composition.

While the hydroxyl group content of the co-polymers may vary slightly over the compositional range considered (as suggested in Table 1), we expect this change to be small in light of the expected changes in co-monomer composition. The pre-polymerization solution composition is given by mass, but the molar composition is more representative of the distribution of hydroxyl groups. For example, in the HEMA:GMA:GMAOH 60:40:0 sample, 62% (by mole) of the side chains have a single hydroxyl group. By comparison, the HEMA:GMA:GMAOH 0:40:60 sample has 37% (by mole) side chains that contain two hydroxyl groups. As such, the hydroxyl groups are highly localized in the HEMA:GMA:GMAOH 0:40:60 sample compared to the HEMA:GMA:GMAOH 60:40:0 sample. While we recognize the possibility for small variations in cross-link density and/or hydroxyl group content of the co-polymers, we believe that the configuration of the hydroxyl groups in the co-polymers primarily influences the resulting material properties, and the subsequent discussion is focused accordingly.

Table 1
Water content and dry polymer density data measured at 22 ± 1 °C. Water content measurements were made on samples initially equilibrated with DI water. The water sorption coefficient, K_w, was taken as equivalent to the volume fraction of water in the material, which was calculated using Equation (3). Co-polymer composition is reported as in Fig. 2. The uncertainty was taken as one standard deviation from the mean of three measurements.

HEMA:GMA:GMAOH Composition (by mass)	Water Uptake [g(water)/g(dry polymer)]	Dry Density (g/cm^3)	K_w	Hydroxyl Group Content [meq(-OH)/g(dry polymer)]
0:60:40	0.24 ± 0.02	1.29 ± 0.02	0.23 ± 0.01	5.0
15:55:30	0.24 ± 0.01	1.30 ± 0.03	0.24 ± 0.01	4.9
30:50:20	0.24 ± 0.01	1.27 ± 0.01	0.23 ± 0.01	4.8
45:45:10	0.23 ± 0.01	1.27 ± 0.01	0.23 ± 0.01	4.7
60:40:0	0.23 ± 0.01	1.26 ± 0.02	0.23 ± 0.01	4.6

Table 2
Salt transport property data for the series of HEMA:GMA:GMAOH materials. The salt sorption coefficient measurements were made at 22 ± 1 °C using sample that initially had been equilibrated with 0.5 mol/L NaCl. Salt permeability was measured at 25 ± 0.2 °C using an upstream salt concentration of 0.5 mol/L NaCl. For each experimentally determined value, the uncertainty was taken as one standard deviation from the mean of three measurements. The apparent salt diffusion coefficient was calculated from the measured salt sorption and salt permeability coefficients using Equation (6), and standard propagation of error [60] was used to estimate the uncertainty in the salt diffusion coefficient. Co-polymer composition is reported as in Fig. 2.

HEMA:GMA:GMAOH Composition (by mass)	K_s	P_s(x 10^{-9} cm^2/s)	D_s(x 10^{-8} cm^2/s)
0:60:40	0.118 ± 0.004	16.2 ± 0.6	13.7 ± 0.1
15:55:30	0.104 ± 0.004	11.6 ± 0.4	11.2 ± 0.1
30:50:20	0.097 ± 0.001	8.7 ± 0.1	9.0 ± 0.1
45:45:10	0.090 ± 0.002	7.0 ± 0.1	7.8 ± 0.1
60:40:0	0.080 ± 0.002	6.0 ± 0.1	7.5 ± 0.1

3.2.1. Salt sorption

Increasing the HEMA content, while simultaneously reducing the GMAOH content of HEMA:GMA:GMAOH, drives a reduction in the salt sorption coefficient or an increase in the ability of the polymer to exclude salt (Table 2). In many hydrated polymers, salt sorption coefficients tend to vary proportionally with the water content of the polymer (i.e., K_s typically increases as K_w increases) [4,19,31]. The cross-linked hydrogel data in Fig. 3 illustrate this type of relationship. Engineering the molecular position of the functional groups in the HEMA:GMA:GMAOH materials, however, allows access to different salt sorption properties without changing the water content of the polymer (Fig. 3).

This result may suggest that adjusting the distribution of a given functional group within a polymer can have a pronounced influence on salt sorption properties. The observed change in the salt sorption coefficient without a corresponding change in water content suggests that the change in functional group configuration affects the thermodynamic environment of the hydrated polymer. As discussed subsequently, we believe that the observed salt sorption properties are highly related to changes in the hydrogen bonding environment within the co-polymer, which can be probed via DSC and microwave dielectric relaxation spectroscopy measurements.

3.2.2. Salt permeability and diffusivity

To further explore the influence of hydroxyl functional group configuration on salt transport, we characterized the salt permeability of the HEMA:GMA:GMAOH materials. Similar to the salt sorption coefficient observations (Fig. 3), the salt permeability decreased as the HEMA content of the co-polymer increased (Fig. 4A). This decrease in salt permeability, P_s, is related to the observed decrease in the salt sorption coefficient, K_s, by the solution-diffusion model where $P_s = K_s \times D_s$ (i.e., Equation (6)) [21].

Unique to this study is the fact that the observed changes in salt sorption and permeability occur at a fixed water content. Several

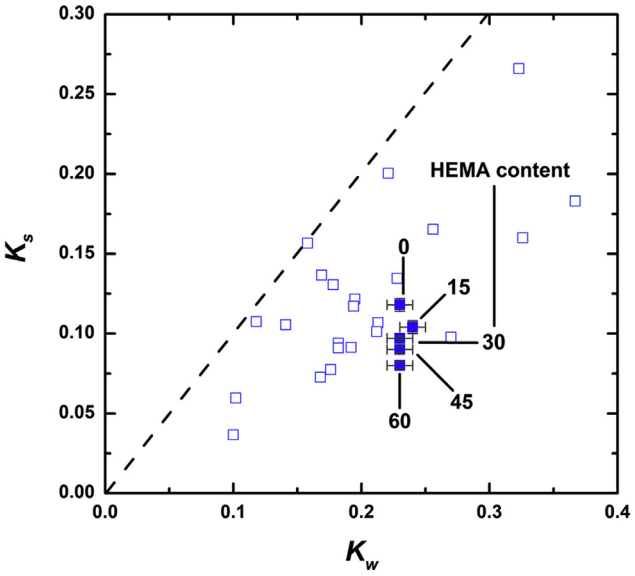

Fig. 3. Salt sorption coefficient data as a function of the water sorption coefficient for HEMA:GMA:GMAOH (this study, ■) and hydrogels (□) [31]. The dashed line on this parity plot indicates the border between salt exclusion from the polymer (points below the line) and salt enrichment in the polymer (points above the line). For HEMA:GMA:GMAOH, the HEMA co-monomer composition of the pre-polymerization solution used to prepare each co-polymer is reported for each data point.

studies have established that water content has a significant impact on salt sorption and permeability properties (e.g., the open symbols in Figs. 3 and 4) [4,5,31]. Our results, however, suggest that the functional group configuration of a polymer (not simply water content alone) can be used to control salt sorption and permeability properties, and this observation suggests new opportunities for membrane science.

Free volume theory provides a framework to explain the dashed line relationships shown in Fig. 4 [4,31,61]. Yasuda proposed a free volume-based model where the water content of the polymer was taken to be proportional to the polymer free volume [31]. This model suggests that the natural logarithms of both the permeability and diffusion coefficients should scale with inverse water content provided that water content is a proxy for free volume and that transport can be described by the free volume model [31]. As such, the natural logarithm of salt permeability and diffusion coefficients tend to decrease linearly with the inverse water sorption coefficient (i.e., $1/K_w$). An example of this relationship is illustrated in Fig. 4A where the salt permeability of several uncharged hydrogels decrease with $1/K_w$. One implication of this model is that movement along the dashed line in Fig. 4A indicates that salt permeability is changing in response to changes in free volume brought about by water content changes in the polymer, i.e., other polymer compositional effects are secondary.

In the HEMA:GMA:GMAOH materials considered in this study, the water content of all 5 samples is statistically indistinguishable, so the

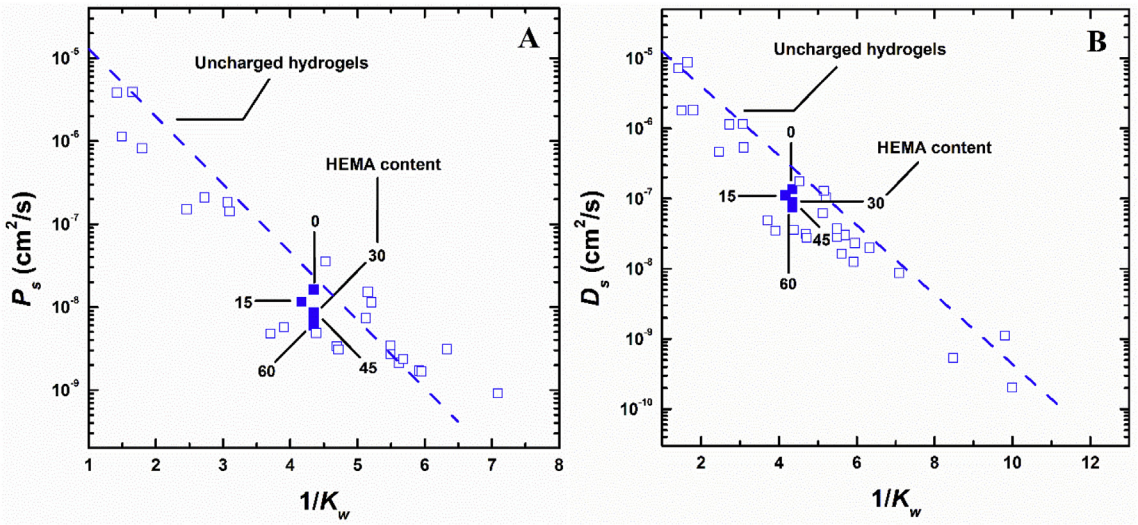

Fig. 4. Salt permeability (A) and apparent salt diffusion (B) coefficients as a function of inverse water sorption coefficient for HEMA:GMA:GMAOH (this study, ■) and hydrogels (□) [31]. For HEMA:GMA:GMAOH, the HEMA co-monomer composition of the pre-polymerization solution used to prepare each co-polymer is reported for each data point. The dashed lines are drawn to guide the eye for the hydrogel data.

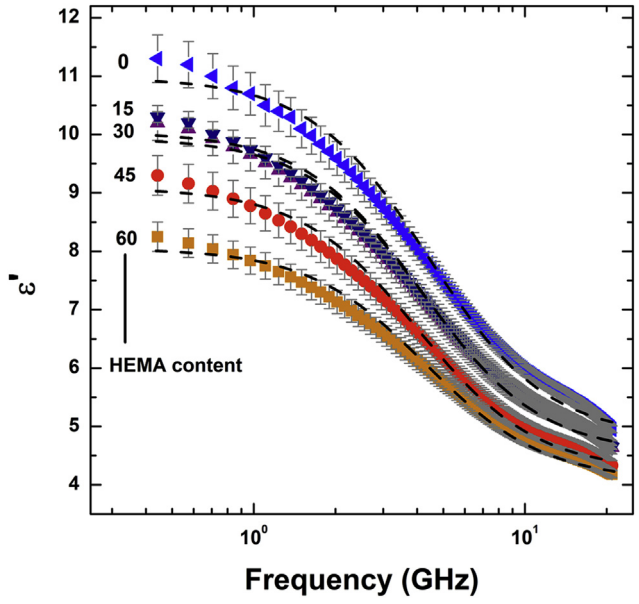

Fig. 5. Frequency-dependent relative permittivity, ε′, data for the HEMA:GMA:GMAOH co-polymers. The data sets are labeled with the HEMA co-monomer composition of the pre-polymerization solution used to prepare each co-polymer. Dashed curves are a single Debye relaxation fit to the measured data. All measurements were made at 22 ± 1 °C, and the uncertainty was taken as one standard deviation from the mean of three measurements.

observed decrease in salt permeability as HEMA content increases is due to factors other than water content. As such, the HEMA:GMA:GMAOH data points in Fig. 4A move vertically downward as HEMA content increases and not along the dashed line, as would be expected if water content was driving the changes in permeability. This unique behavior is a result of changing the functional group configuration within the polymer.

A similar trend is observed when the salt sorption and permeability coefficients are used to calculate apparent salt diffusion coefficients that can also be plotted versus $1/K_w$ (Fig. 4B). We observed a decrease in the apparent salt diffusion coefficient as HEMA content increased at equivalent water content (Table 1, Fig. 4B), and the decrease was 1.5 times less than the decrease in salt permeability for these HEMA:GMA:GMAOH materials. This result is expected because the decrease in both salt sorption and diffusion coefficients contribute to the overall decrease in salt permeability, according to the solution-diffusion model ($P_s = K_s \times D_s$).

Additionally, we compared the apparent salt diffusion coefficients of HEMA:GMA:GMAOH to those values for other cross-linked hydrogels [31]. At similar water content values (i.e., similar values of $1/K_w$), the magnitudes of the salt diffusivity are similar among these chemically similar materials (Fig. 4B). This observation suggests that molecular motions are similarly facilitated by comparable amounts of sorbed water in these materials.

The hydroxyl group configuration in the HEMA:GMA:GMAOH materials influences salt sorption, diffusivity, and permeability. Investigating this effect using materials of comparable water content reveals unique structure property relationships. Distributing the hydroxyl groups more evenly throughout the polymer (i.e., on the HEMA side chain versus the vicinal diol of the GMAOH side chain) appears to suppress salt sorption and diffusion coefficients. This result may suggest more broadly that distributed hydrophilic functionality may be advantageous for desalination membrane materials.

3.3. Microwave dielectric relaxation spectroscopy

To further explore the underpinnings of the salt transport property results discussed in the previous section, we characterized the dielectric properties of the hydrated HEMA:GMA:GMAOH co-polymers. We performed the analysis in the microwave frequency range where dipolar relaxation motions of water molecules can be probed [45,62–66]. The relative permittivity properties of these materials provide insight into the thermodynamic environment of the polymer and, thus, salt sorption properties [19,24,25,67–71].

We fit the HEMA:GMA:GMAOH relative permittivity data (Fig. 5) to a single Debye relaxation process to determine the static permittivity (i.e., static dielectric constant) of the material [23,72]. Though the single Debye relaxation model is likely an oversimplified description of dipolar relaxations in these hydrated polymers (i.e., agreement between the data and the single Debye relaxation is not perfect), this approach provides a uniform method to approximate the static permittivity properties (i.e., the value of the ε′ plateau at low frequency) of the materials [23]. The static permittivity is useful for quantifying the extent of water dipole relaxation and for modeling ion sorption thermodynamics in hydrated polymers [19,23,24].

The single Debye relaxation fitting process revealed that the static permittivity values of the HEMA:GMA:GMAOH materials decreased from 11.0, 10.0, 9.9, 9.1, to 8.1 as HEMA content increased from 0, 15, 30, 45, to 60%. It is important to note, again, that the water content of all of the co-polymers was statistically indistinguishable. This result is consistent with previous work suggesting that polymer chemistry (and not water content alone) plays an important role in determining the dielectric properties of hydrated polymers [23].

The observed decrease in the magnitude of the relative permittivity and the regressed static permittivity properties as the HEMA content of the co-polymer increased could be interpreted as a reduction in the dielectric constant of the co-polymer as HEMA content increases. Consistent with electrostatic theory, lower dielectric constant materials often exclude salt to a greater extent than higher dielectric constant materials [19,23]. As such, the relative permittivity data shown in Fig. 5 are qualitatively consistent with the salt sorption data reported in Table 2 as the relative permittivity and salt sorption coefficient decreased as the HEMA content of HEMA:GMA:GMAOH increased.

Another molecular interpretation of the data in Fig. 5 is that dipolar relaxation processes are weaker, or less energy is dissipated during the dipolar relaxations, in materials that contain more HEMA co-monomer. We believe this result may suggest that transitioning from a vicinal diol-based co-polymer to a system where hydroxyl groups are more distributed throughout the polymer matrix may have the effect of slowing water molecule motions within the hydrated co-polymer. This result is also consistent with the observed reduction in salt diffusion coefficient values as the HEMA content of the co-polymer increases (Fig. 4B).

3.4. State of water analysis

The dielectric permittivity data discussed in the previous section suggest that different states of water may exist within the co-polymers and mobility of sorbed water in each sample may be affected by the configuration of hydroxyl groups in the polymer. Several studies have investigated the state of water in hydrated polymers [23,48–55,64,73]. Many of these studies use differential scanning calorimetry to quantify the state of water in hydrated polymers, and we applied that approach to the HEMA:GMA:GMAOH materials.

All of the thermograms for the HEMA:GMA:GMAOH co-polymers (Fig. 6) indicated the presence of freezable sorbed water (i.e., we observed a melting transition at 0 °C for each material). We calculated the amount of freezable and non-freezable water sorbed in the co-polymers, and freezable water content decreased from 2.3 to 0.9% as HEMA content increased (Table 3). Non-freezable water content remained similar among all of the co-polymers (Table 3) presumably because the concentration of hydroxyl groups only decreased slightly as HEMA content increased (Table 1).

State of water analysis suggests that materials with more HEMA had less freezable water than the materials containing more GMAOH. As such, the more distributed hydroxyl group configuration in the HEMA-rich materials may promote stronger water-polymer interactions. These interactions could reduce the likelihood of forming water clusters that contain freezable (or bulk-like) water; such clusters may be more favorable in the vicinal diol-rich materials that contain more GMAOH compared to HEMA. Formation of such bulk-like water clusters may reduce transport selectivity, so engineering materials to have more distributed functional groups throughout the polymer matrix may favor transport selectivity, which is critical for desalination applications [11,57].

The decrease in the HEMA:GMA:GMAOH apparent salt diffusion coefficient with increasing HEMA content (Fig. 4B) may be the result of less freezable water (i.e., bulk-like water) clustering around the hydroxyl groups in the HEMA-rich materials. To illustrate this point, we calculated the freezable (i.e., bulk-like) water content per equivalent of hydroxyl group in the co-polymers, and increasing the HEMA content of the pre-polymerization solution from 0% to 60% by mass caused the amount of freezable water, in the co-polymer film, per equivalent of hydroxyl group to decrease by more than a factor of 2 (See the Supplementary Information for additional details). This result suggests that freezable water content may be suppressed by preparing polymers with more distributed hydrophilic functional groups. Such a situation could also result in more tortuous transport pathways [23,74], which could impact salt diffusivity properties.

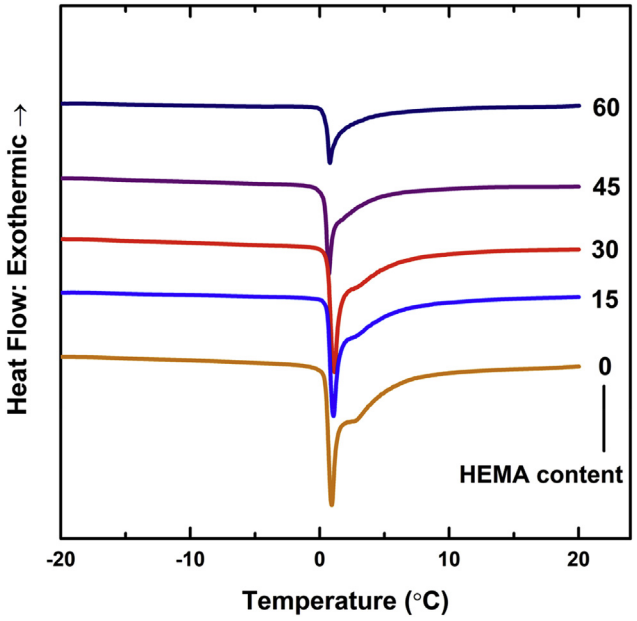

Fig. 6. Differential scanning calorimetry (DSC) thermograms for the hydrated GMA:HEMA:GMAOH materials. The HEMA co-monomer composition of the pre-polymerization solution used to prepare each co-polymer is reported for each data set.

Table 3
The distribution of freezable and non-freezable water in the HEMA:GMA:GMAOH materials was calculated using water uptake (Table 1) and DSC data. The sum of w_f and w_{nf} is equivalent to the total water uptake of the material. The co-polymer composition is reported as in Fig. 2.

HEMA:GMA:GMAOH Composition (by mass)	W_f (%)	W_{nf} (%)
0:60:40	2.3	21.2
15:55:30	1.9	22.3
30:50:20	1.8	21.7
45:45:10	1.2	22.3
60:40:0	0.9	22.4

Additionally, the state of water results are consistent with the dielectric permittivity analysis (Fig. 5) as they provide quantitative insight into the lower static permittivity of higher HEMA content materials. A more evenly distributed hydroxyl group configuration may allow water to interact with the polymer backbone to a greater extent, and this situation could reduce freezable water content compared to the situation where hydroxyl groups are situated closer together (i.e., the GMAOH-rich materials). In other polymers, freezable water content and relative permittivity properties appear to be related [23], so the simultaneous reduction in freezable water content and relative permittivity observed in these materials, as HEMA content increases, is consistent with previously observed phenomena.

This study focused on salt transport properties, but water transport properties are also important for desalination applications. The water permeability, like salt permeability, can be described using the solution diffusion model (i.e., water permeability is taken as the product of the water sorption coefficient and an apparent water diffusion coefficient)

[21,22]. The slowing of water molecule motions, suggested by the dielectric permittivity data and state of water analysis presented here, cause a decrease in the apparent water diffusion coefficient reported in a separate study [57]. Importantly, however, the water sorption coefficient (unlike the salt sorption coefficient) remains constant as the HEMA content of the co-polymer increases. Therefore, the salt permeability decreases to a greater extent than the water permeability. As such, the water/salt selectivity, which is coupled to salt rejection and important for desalination applications, increases as the co-polymer composition shifts from the vicinal diol-rich material to the HEMA-rich co-polymer with more evenly distributed hydroxyl groups [57].

4. Conclusions

The molecular configuration of hydroxyl groups in a series of equivalent water content methacrylate-based HEMA:GMA:GMAOH co-polymers influences salt transport properties. Shifting from a vicinal diol-rich hydroxyl group configuration (GMAOH-rich co-polymer) to a configuration where only a single hydroxyl group is present on the co-polymer side chain (HEMA-rich co-polymer) leads to a reduction in salt sorption and permeability coefficients, which is favorable for desalination membrane applications. The observed reduction in salt sorption, as the HEMA content of the co-polymer increases, is consistent with a simultaneous reduction in the relative permittivity (or dielectric constant) and the freezable water content of the hydrated co-polymer. A reduction in the apparent salt diffusion coefficient as the HEMA content of the co-polymer increases is also consistent with a hydrogen bonding environment where water molecules interact to a greater extent with the polymer backbone, and both of these conditions are consistent with the observed reduction in relative permittivity and freezable water content as the HEMA content of the co-polymer increased. These results suggest that salt transport properties can be engineered by exercising molecular control over functional group position in hydrated polymers. The results suggest that a more distributed functional group configuration may facilitate low rates of salt transport, which could be a viable strategy for preparing water/salt selective polymers for desalination membrane applications.

Acknowledgements

This material is based upon work supported in part by the National Science Foundation under Grant No. CBET-1752048. The authors also acknowledge support from the Oak Ridge Associated Universities (ORAU) Ralph E. Powe Junior Faculty Award and from the Volkswagen Group of North America Fellowship.

Appendix A. Supplementary data

Supplementary data to this article can be found online at https://doi.org/10.1016/j.memsci.2019.117295.

References

[1] Y. Cohen, R. Semiat, A. Rahardianto, A perspective on reverse osmosis water desalination: quest for sustainability, AIChE J. 63 (2017) 1771–1784.
[2] M. Elimelech, W.A. Phillip, The future of seawater desalination: energy, technology, and the environment, Science 333 (2011) 712–717.
[3] M.A. Shannon, P.W. Bohn, M. Elimelech, J.G. Georgiadis, B.J. Marinas, A.M. Mayes, Science and technology for water purification in the coming decades, Nature 452 (2008) 301–310.
[4] G.M. Geise, D.R. Paul, B.D. Freeman, Fundamental water and salt transport properties of polymeric materials, Prog. Polym. Sci. 39 (2014) 1–42.
[5] G.M. Geise, H.-S. Lee, D.J. Miller, B.D. Freeman, J.E. McGrath, D.R. Paul, Water purification by membranes: the role of polymer science, J. Polym. Sci. B Polym. Phys. 48 (2010) 1685–1718.
[6] J. Kamcev, B.D. Freeman, Charged polymer membranes for environmental/energy applications, Ann. Rev. Chem. Biomol. Eng. 7 (2016) 111–133.
[7] C. Fritzmann, J. Löwenberg, T. Wintgens, T. Melin, State-of-the-art of reverse osmosis desalination, Desalination 216 (2007) 1–76.
[8] R.F. Service, Desalination freshens up, Science 313 (2006) 1088–1090.
[9] R. Semiat, Energy issues in desalination processes, Environ. Sci. Technol. 42 (2008) 8193–8201.
[10] S. Miller, H. Shemer, R. Semiat, Energy and environmental issues in desalination, Desalination 366 (2015) 2–8.
[11] J.R. Werber, A. Deshmukh, M. Elimelech, The critical need for increased selectivity, not increased water permeability, for desalination membranes, Environ. Sci. Technol. Lett. 3 (2016) 112–120.
[12] H.B. Park, J. Kamcev, L.M. Robeson, M. Elimelech, B.D. Freeman, Maximizing the right stuff: the trade-off between membrane permeability and selectivity, Science (2017) 356 eaab0530.
[13] D.M. Stevens, J.Y. Shu, M. Reichert, A. Roy, Next-generation nanoporous materials: progress and prospects for reverse osmosis and nanofiltration, Ind. Eng. Chem. Res. 56 (2017) 10526–10551.
[14] S. Surawanvijit, A. Rahardianto, Y. Cohen, An integrated approach for characterization of polyamide reverse osmosis membrane degradation due to exposure to free chlorine, J. Membr. Sci. 510 (2016) 164–173.
[15] T. Knoell, Municipal Wastewater: Chlorine's Impact on the Performance and Properties of Polyamide Membranes, Ultrapure Water, 2006, pp. 24–31.
[16] H.B. Park, B.D. Freeman, Z.-B. Zhang, M. Sankir, J.E. McGrath, Highly chlorine-tolerant polymers for desalination, Angew. Chem. Int. Ed. 47 (2008) 6019–6024.
[17] A.E. Allegrezza, B.S. Parekh, P.L. Parise, E.J. Swiniarski, J.L. White, Chlorine resistant polysulfone reverse osmosis modules, Desalination 64 (1987) 285–304.
[18] S.G. Kimura, Reverse osmosis performance of sulfonated poly(2,6-dimethylphenylene ether) ion exchange membranes, Ind. Eng. Chem. Res. 10 (1971) 335–339.
[19] H. Zhang, G.M. Geise, Modeling the water permeability and water/salt selectivity tradeoff in polymer membranes, J. Membr. Sci. 520 (2016) 790–800.
[20] G.M. Geise, L.P. Falcon, B.D. Freeman, D.R. Paul, Sodium chloride sorption in sulfonated polymers for membrane applications, J. Membr. Sci. 423 (2012) 195–208.
[21] J.G. Wijmans, R.W. Baker, The solution-diffusion model: a review, J. Membr. Sci. 107 (1995) 1–21.
[22] D.R. Paul, Reformulation of the solution-diffusion theory of reverse osmosis, J. Membr. Sci. 241 (2004) 371–386.
[23] K. Chang, H. Luo, G.M. Geise, Water content, relative permittivity, and ion sorption properties of polymers for membrane desalination, J. Membr. Sci. 574 (2019) 24–32.
[24] A.E. Yaroshchuk, Dielectric exclusion of ions from membranes, Adv. Colloid Interface Sci. 85 (2000) 193–230.
[25] A.E. Yaroshchuk, Non-steric mechanisms of nanofiltration: superposition of Donnan and dielectric exclusion, Separ. Purif. Technol. 22–23 (2001) 143–158.
[26] K. Chang, T. Xue, G.M. Geise, Increasing salt size selectivity in low water content polymers via polymer backbone dynamics, J. Membr. Sci. 552 (2018) 43–50.
[27] K. Chang, A. Korovich, T. Xue, W.A. Morris, L.A. Madsen, G.M. Geise, Influence of rubbery versus glassy backbone dynamics on multiscale transport in polymer membranes, Macromolecules 51 (2018) 9222–9233.
[28] H. Luo, J. Aboki, Y. Ji, R. Guo, G.M. Geise, Water and salt transport properties of triptycene-containing sulfonated polysulfone materials for desalination membrane applications, ACS Appl. Mater. Interfaces 10 (2018) 4102–4112.
[29] M.A. Hickner, Ion-containing polymers: new energy & clean water, Mater. Today 13 (2010) 34–41.
[30] J.S. Mackie, P. Meares, The diffusion of electrolytes in a cation-exchange resin membrane I. Theoretical, Proc. R. Soc. Lond. Ser A Math. Phys. Sci. 232 (1955) 498–509.
[31] H. Yasuda, C.E. Lamaze, L.D. Ikenberry, Permeability of solutes through hydrated polymer membranes. Part I. Diffusion of sodium chloride, Makromol. Chem. 118 (1968) 19–35.
[32] H. Yasuda, C.E. Lamaze, A. Peterlin, Diffusive and hydraulic permeabilities of water in water-swollen polymer membranes, J. Polym. Sci. A-2 Polym. Phys. 9 (1971) 1117–1131.
[33] J. Tan, D. Liu, Y. Bai, C. Huang, X. Li, J. He, Q. Xu, X. Zhang, L. Zhang, An insight into aqueous photoinitiated polymerization-induced self-assembly (photo-PISA) for the preparation of diblock copolymer nano-objects, Polym. Chem. 8 (2017) 1315–1327.
[34] W. Brostow, R. Chiu, I.M. Kalogeras, A. Vassilikou-Dova, Prediction of glass transition temperatures: binary blends and copolymers, Mater. Lett. 62 (2008) 3152–3155.
[35] T.G.J. Fox, P.J. Flory, Second-order transition temperatures and related properties of polystyrene. I. Influence of molecular weight, J. Appl. Phys. 21 (1950) 581–591.
[36] P.C. Hiemenz, T.P. Lodge, Polymer Chemistry, second ed., CRC Press LLC, Boca Raton, Florida, 2007.
[37] D. Halliday, R. Resnick, J. Walker, Fundamentals of Physics, seventh ed., Wiley, Hoboken, New Jersey, 2005.
[38] H. Ju, A.C. Sagle, B.D. Freeman, J.I. Mardel, A.J. Hill, Characterization of sodium chloride and water transport in crosslinked poly(ethylene oxide) hydrogels, J. Membr. Sci. 358 (2010) 131–141.
[39] J. Rumble, CRC Handbook of Chemistry and Physics, 98th ed., CRC Press LLC, Boca Raton, Florida, 2017.
[40] C.L. Yaws, R.W. Pike, Thermophysical Properties of Chemicals and Hydrocarbons, William Andrew, Norwich, New York, 2009.
[41] G.M. Geise, C.L. Willis, C.M. Doherty, A.J. Hill, T.J. Bastow, J. Ford, K.I. Winey, B.D. Freeman, D.R. Paul, Characterization of aluminum-neutralized sulfonated styrenic pentablock copolymer films, Ind. Eng. Chem. Res. 52 (2013) 1056–1068.
[42] E.L. Cussler, Diffusion: Mass Transfer in Fluid Systems, third ed., Cambridge University Press, Cambridge, New York, 2009.
[43] G.M. Geise, B.D. Freeman, D.R. Paul, Characterization of a sulfonated pentablock

copolymer for desalination applications, Polymer 51 (2010) 5815–5822.
[44] L.F. Chen, Microwave Electronics: Measurement and Materials Characterization, Wiley, Hoboken, New Jersey, 2004.
[45] Z. Lu, M. Lanagan, E. Manias, D.D. Macdonald, Two-port transmission line technique for dielectric property characterization of polymer electrolyte membranes, J. Phys. Chem. B 113 (2009) 13551–13559.
[46] P.G. Bartley, S.B. Begley, A new technique for the determination of the complex permittivity and permeability of materials, IEEE Instrumentation & Measurement Technology Conference Proceedings, 2010, pp. 54–57.
[47] T.A. Instruments, Purge Gas Recommendations for Use in Modulated DSC®, http://www.tainstruments.com/pdf/literature/TN44.pdf June 13th, 2018.
[48] S.J. Paddison, Proton conduction mechanisms at low degrees of hydration in sulfonic acid–based polymer electrolyte membranes, Annu. Rev. Mater. Res. 33 (2003) 289–319.
[49] K.A. Mauritz, R.B. Moore, State of understanding of Nafion®, Chem. Rev. 104 (2004) 4535–4586.
[50] K.-D. Kreuer, S.J. Paddison, E. Spohr, M. Schuster, Transport in proton conductors for fuel-cell applications: Simulations, elementary reactions, and phenomenology, Chem. Rev. 104 (2004) 4637–4678.
[51] J.A. Elliott, S.J. Paddison, Modelling of morphology and proton transport in PFSA membranes, Phys. Chem. Chem. Phys. 9 (2007) 2602–2618.
[52] F.X. Quinn, E. Kampff, G. Smyth, V.J. McBrierty, Water in hydrogels. 1. A study of water in poly(N-vinyl-2-pyrrolidone/methyl methacrylate) copolymer, Macromolecules 21 (1988) 3191–3198.
[53] R.M. Hodge, T.J. Bastow, G.H. Edward, G.P. Simon, A.J. Hill, Free volume and the mechanism of plasticization in water-swollen poly(vinyl alcohol), Macromolecules 29 (1996) 8137–8143.
[54] H. Yoshida, Y. Miura, Behavior of water in perfluorinated ionomer membranes containing various monovalent cations, J. Membr. Sci. 68 (1992) 1–10.
[55] N. Shinyashiki, M. Shimomura, T. Ushiyama, T. Miyagawa, S. Yagihara, Dynamics of water in partially crystallized polymer/water mixtures studied by dielectric spectroscopy, J. Phys. Chem. B 111 (2007) 10079–10087.
[56] T.A. Instruments, Thermal Analysis to Determine Various Forms of Water Present in Hydrogels, http://www.tainstruments.com/pdf/literature/TA384.pdf June 12th, 2018.
[57] H. Luo, K. Chang, K. Bahati, G.M. Geise, Engineering selective desalination membranes via molecular control of polymer functional groups, Environ. Sci. Technol. Lett. (2019), https://doi.org/10.1021/acs.estlett.9b00351.
[58] R.F. Lama, B.C.Y. Lu, Excess thermodynamic properties of aqueous alcohol solutions, J. Chem. Eng. Data 10 (1965) 216–219.
[59] D.V. Batov, A.M. Zaichikov, V.P. Slyusar, V.P. Korolev, Enthalpies of mixing and state of components in aqueous-organic mixtures with nets of hydrogen bonds, Russ. J. Gen. Chem. 71 (2001) 1208–1214.
[60] P.R. Bevington, D.K. Robinson, Chapter 4: propagation of errors, Data Reduction and Error Analysis for the Physical Sciences, McGraw Hill, New York, 2003, pp. 56–65.
[61] W. Xie, H. Ju, G.M. Geise, B.D. Freeman, J.I. Mardel, A.J. Hill, J.E. McGrath, Effect of free volume on water and salt transport properties in directly copolymerized disulfonated poly(arylene ether sulfone) random copolymers, Macromolecules 44 (2011) 4428–4438.
[62] S.J. Paddison, D.W. Reagor, T.A. Zawodzinski Jr., High frequency dielectric studies of hydrated Nafion®, J. Electroanal. Chem. 459 (1998) 91–97.
[63] S. Paddison, G. Bender, T.A. Zawodzinski Jr., The microwave region of the dielectric spectrum of hydrated Nafion® and other sulfonated membranes, J. New Mater. Electrochem. Syst. 3 (2000) 293–302.
[64] Z. Lu, G. Polizos, D.D. Macdonald, E. Manias, State of water in perfluorosulfonic ionomer (Nafion® 117) proton exchange membranes, J. Electrochem. Soc. 155 (2008) B163–B171.
[65] Z. Lu, E. Manias, D.D. Macdonald, M. Lanagan, Dielectric relaxation in dimethyl sulfoxide/water mixtures studied by microwave dielectric relaxation spectroscopy, J. Phys. Chem. A 113 (2009) 12207–12214.
[66] G. Smith, A.P. Duffy, J. Shen, C.J. Olliff, Dielectric relaxation spectroscopy and some applications in the pharmaceutical sciences, J. Pharm. Sci. 84 (1995) 1029–1044.
[67] E. Glueckauf, On the mechanism of osmotic desalting with porous membranes, Proceedings of the First International Symposium on Water Desalination (1967) 143–150.
[68] J.E. Anderson, W. Pusch, The membrane/water partition coefficients of ions: electrostatic calculations of dielectric heterogeneity, Ber. Bunsen Ges. Phys. Chem. 80 (1976) 846–849.
[69] V. Freger, S. Bason, Characterization of ion transport in thin films using electrochemical impedance spectroscopy: I. Principles and theory, J. Membr. Sci. 302 (2007) 1–9.
[70] J. Kamcev, M. Galizia, F.M. Benedetti, E.-S. Jang, D.R. Paul, B.D. Freeman, G.S. Manning, Partitioning of mobile ions between ion exchange polymers and aqueous salt solutions: importance of counter-ion condensation, Phys. Chem. Chem. Phys. 18 (2016) 6021–6031.
[71] J. Kamcev, D.R. Paul, G.S. Manning, B.D. Freeman, Predicting salt permeability coefficients in highly swollen, highly charged ion exchange membranes, ACS Appl. Mater. Interfaces 9 (2017) 4044–4056.
[72] Z. Lu, State of water in perfluorosulfonic acid membranes studied by microwave dielectric relaxation spectroscopy, Ph.D. Thesis, Department of Materials Science and Engineering, the Pennsylvania State University, University Park, Pennsylvania, 2006.
[73] T. Tran, C. Lin, S. Chaurasia, H. Lin, Elucidating the relationship between states of water and ion transport properties in hydrated polymers, J. Membr. Sci. 574 (2019) 299–308.
[74] K.D. Kreuer, On the development of proton conducting polymer membranes for hydrogen and methanol fuel cells, J. Membr. Sci. 185 (2001) 29–39.